



## Research Article

# Development and Characterization of a Novel Spray-Dried Powder for Inhalation of Cinacalcet HCl Nanoparticles

Katayoon Mireskandari<sup>1,2</sup>, Mostafa Rostamnezhad<sup>1</sup>, Majid Darabi<sup>1</sup>, Mohammadreza Rouini<sup>1,2</sup>, Alireza Vatanara<sup>1</sup>

<sup>1</sup>Department of Pharmaceutics, Faculty of Pharmacy, Tehran University of Medical Sciences, Tehran, Iran.

<sup>2</sup>Biopharmaceutics and Pharmacokinetic Division, Department of Pharmaceutics, School of Pharmacy, Tehran University of Medical Sciences, Tehran, Iran.

## Article Info

### Article History:

Received: 4 Sep 2023

Accepted: 13 Dec 2023

ePublished: 25 Jan 2024

### Keywords:

- Cinacalcet HCl
- Dissolution profile
- Dry powder inhalation
- Nanosuspension
- Solubility
- Sonoprecipitation

## Abstract

**Background:** Administering Cinacalcet HCl (CINA) can be challenging because of its low oral bioavailability (20 to 25%) due mainly to its high first-pass metabolism and poor aqueous solubility. However, nanosuspensions are an effective way of enhancing solubility by reducing size. Furthermore, pulmonary delivery of the drug as a promising alternative route can bypass the hepatic first-pass metabolism.

**Methods:** A CINA nanosuspension was produced by sonoprecipitation and optimized to achieve minimum particle size and polydispersity index (PDI). These nanosuspensions were then spray-dried with different types of sugars to form nano-in-micro composite particles. The particles were then analyzed by scanning electron microscopy (SEM), X-ray diffraction (XRD), Fourier transform infrared (FTIR), and differential scanning calorimetry (DSC), and the dissolution rate, solubility, and in vitro aerosol deposition behavior were determined.

**Results:** The particle size of nanosuspensions was in the range of 239.5 to 1281.8 nm and the size was dependent on the process parameters. The spray-dried microparticles had a smooth and spherical surface morphology. The particle size of the composite particles was in the range of 2 to 10  $\mu\text{m}$  and the dissolution rate of processed powders was significantly higher than raw CINA powder. Its crystallinity was partially diminished and no polymorphic conversion were observed. The in vitro deposition study, using a twin-stage impinger (TSI), presented fine particle fractions up to 76.7 percent.

**Conclusion:** The utilization of nano-in-micro composite particles as a pulmonary delivery system for CINA has shown great potential in enabling a more efficient drug delivery.

## Introduction

There has been a significant emphasis on the use of the pulmonary route for systemic drug delivery, primarily because the respiratory system offers a non-invasive method of providing some drug substances.<sup>1-3</sup> By preventing degradation in the gastrointestinal tract, inhalation devices require lower drug dosages for equivalent therapeutic efficacy compared to oral administration.<sup>4</sup> Furthermore, the lungs have a high degree of vascularization, which allows for rapid drug absorption without requiring hepatic first-pass effects and relatively low local metabolic activity.<sup>3,4</sup>

Secondary hyperparathyroidism (SHPT) is a common condition among individuals with chronic kidney disease (CKD). It affects almost all CKD patients who have reached end-stage renal disease and require dialysis. In patients undergoing dialysis, severe SHPT is associated with a 20% higher mortality rate. This may be due to an increased risk of extra-skeletal calcification and fractures, which can lead

to cardiovascular disease.<sup>5</sup>

Cinacalcet hydrochloride (CINA) is the first type 2 calcimimetic molecule introduced to the market. It decreases concentrations of parathyroid hormone and serum calcium by increasing sensitivity of calcium-sensing receptors in the parathyroid gland. CINA is approved for the treatment of secondary hyperparathyroidism in patients on dialysis with chronic kidney disease (CKD) and in patients with parathyroid carcinoma.<sup>6,7</sup> It has been reported that CINA could considerably reduce the number of parathyroidectomy surgeries.<sup>8</sup> The most frequent side effects of CINA are nausea and vomiting, experienced by about 30% of the patients.<sup>9</sup> Over time, these side effects reduce medication adherence in patients, particularly in dialysis patients who have poor medication adherence.<sup>10</sup> GI events occurring in hemodialysis patients under treatment with CINA may be related to inhibiting or delaying gastric emptying. Abnormal GI motility might be a principal mechanism of GI events and a good marker of

\*Corresponding Author: Alireza Vatanara, E-mail: [vatanara@tums.ac.ir](mailto:vatanara@tums.ac.ir)

©2024 The Author(s). This is an open access article and applies the Creative Commons Attribution Non-Commercial License (<http://creativecommons.org/licenses/by-nc/4.0/>). Non-commercial uses of the work are permitted, provided the original work is properly cited.

side effects in the GI tract. It was shown that the required dose of CINA for a significant PTH reduction in rats was around 30 times the dose that caused inhibition of gastric emptying.<sup>11</sup>

As per the Biopharmaceutical Classification System (BCS), CINA is categorized as Class IV due to its low water solubility. The bioavailability of CINA is about 20 to 25%, suggesting a high first-pass metabolism.<sup>12</sup> It does not have dose proportionality and shows irreproducible clinical responses. Several formulation techniques have been utilized to increase the drug's solubility and rate of dissolution. Different delivery systems of CINA in the forms of self-micro-emulsifying drug delivery system,<sup>13</sup> self-nano emulsifying drug delivery system,<sup>14</sup> nanocrystals (NCs),<sup>15</sup> solid lipid nanoparticles (SLN),<sup>16</sup> and/or nano-emulsion have been studied.<sup>17</sup> Still, these formulations have yet to be introduced to the market. The Noyes-Whitney equation<sup>18</sup> indicates that increasing a drug's specific surface area and decreasing its particle size is one way of accelerating its dissolution rate and potentially solving the bioavailability issue. To enhance the dissolving rate, several methods, comprising high-pressure homogenization, precipitation technique, and wet medium milling, could be applied to develop drug nanoparticles.<sup>19,20</sup>

Nevertheless, due to their increased Brownian motion, comparatively large specific surface area, and high surface energy at the nanoscale, nanoparticles have a greater tendency to aggregate.<sup>21</sup> Although different types of stabilizers are used in formulations of nanoparticles, aggregation and particle enlargement may occur by Ostwald ripening gradually during the shelf-life.<sup>22</sup> Additionally, CINA is present in nanoparticles in the amorphous state, which is thermodynamically less stable in comparison to the crystalline CINA. Therefore, crystalline transformation can also destabilize the nanosuspensions.<sup>21,23,24</sup> Among various methods to overcome nanosuspension instability, solidification is the most common method.<sup>25,26</sup> Solidifying nanoparticles have advantages over nanosuspensions in aqueous form due to the substantial reduction in destabilizing processes, including aggregation. Nanosuspensions are frequently converted into a solid state and then formulated into appropriate pharmaceutical forms.<sup>27-29</sup> The pharmaceutical industry often employs spray drying as a technique to transform nanosuspensions into dried particles because it is a time and energy-efficient method.<sup>21,30</sup>

Inhalation drug administration is an alternative to oral administration, which can provide higher bioavailability compared to the oral route. Using nanoparticles in pulmonary drug delivery enhances the rate of drug dissolution and ensures consistent distribution of the drug dosage in the alveoli. This makes it an attractive approach for drug delivery.<sup>31</sup> Additionally, inhaled nanoparticle delivery methods reduce drug loss due to extra-thoracic deposition by minimizing deposition in the mouth-throat region.<sup>32</sup> Delivering drugs via the pulmonary route may also reduce GI side effects by decreasing the systemic and GI exposure

of the drug substance. Given the increasing interest in dry powder inhalations (DPIs) for systemic delivery through the lungs, this dosage form is an excellent candidate to improve the bioavailability of CINA and therefore increase its effectiveness in patients with CKD on dialysis. Among all variables influencing the spray-dried particle quality, employing suitable excipients is essential to obtaining the desired aerodynamic behavior and full redispersion of the nanoparticles into the pre-drying state.<sup>33,34</sup> In addition to functioning as protectors throughout the spray drying and preventing agglomeration, sugars are popular excipients that can help produced powders breathe easier.<sup>25,35</sup> To enhance the drug dissolution rate, the present investigation intended to optimize the preparation of CINA nanosuspension using the antisolvent precipitation-ultrasonication method. In addition, it developed a spray drying method for converting CINA nanosuspension into a stable dry powder by selecting the most suitable sugar and its ratio as an excipient to achieve a powder with the best dissolution quality. The *in vitro* experiments were carried out to assess the solubility and dissolution profile of dried CINA nanocomposite particles. The spray-dried powder was then utilized as a DPI intended for inhalation. In addition, the aerodynamic properties of this nanocomposite particle have been investigated with a twin-stage impinger (TSI).

## Methods

### Materials

CINA was purchased from Dr. Abidi Pharmaceutical Co (Iran). Lactose monohydrate, trehalose, mannitol, raffinose, disodium hydrogen phosphate, dichloromethane (DCM), Lecithin, Poloxamer 188, Polysorbate 80, sodium dodecyl sulfate (SDS), and HPLC grade methanol and acetonitrile were purchased from Merck (Germany). Deionized water was produced by a Milli-Q water purification system (Millipore Co., Ltd., USA) for chromatographic application.

### Quantification of CINA (HPLC method)

Determination of the drug was performed using an HPLC system (Azura, Knauer, Germany) equipped with an ultraviolet detector. The chromatographic separations were performed on a C18 column (150 mm × 4.6 mm inner diameter, and particle size of 5 µm) (Mediterraneasea, Teknokroma, Spain) at (25 ± 2) °C. Separations were performed in the isocratic mode with a flow rate of 1 mL/min of a mobile phase consisting of aqueous phosphate buffer (12.5 mM disodium phosphate in purified water): acetonitrile (19:81, v/v) pH was adjusted to 7.4 using orthophosphoric acid 85% at. The UV detection wavelength was 223 nm.

### Preparation of CINA nanosuspension

To develop CINA nanosuspensions, a modified version of the antisolvent precipitation-ultrasonication technique mentioned in the literature was used.<sup>36</sup> Briefly, in this technique, distilled water was used as the anti-solvent

phase, whereas specific concentrations of CINA were dissolved in DCM to form the organic phase. Different types of stabilizers were examined in both aqueous and organic phases, and lecithin was selected and dissolved in the organic phase along with CINA. To eliminate any particle contaminants, the solutions were passed through a 0.45 µm filter. At a constant temperature, the organic solution was delicately injected dropwise into the anti-solvent employing a syringe. At the same time, a high shear homogenizer (IKA®, T25 digital Ultra-Turrax, Germany) was turned on at 11000 rpm for 5 minutes to obtain a set volume ratio of the aqueous phase to the organic phase.

Box-Behnken design (BBD) was used alongside Design-Expert® 11.0.3.0 software (Stat-ease®, USA) to formulate and optimize nanoparticles (Table 1). The experimental design comprised three independent variables: the concentration of CINA in the organic phase (A), the concentration of stabilizer (B), and the volume ratio of the aqueous to organic phases (C). All experiments were conducted three times, and the average particle size (R1) and polydispersity index (R2) for particles produced in triplicate were recorded and utilized for modeling and optimization. Means and standard deviations for each outcome were provided and a 95% confidence interval was used for a one-way analysis of variance (ANOVA) to determine statistical significance.

### Spray drying of CINA nanosuspension

According to the formulas presented in Table 2, freshly made CINA nanosuspensions were combined with 5 mL of a sugar solution (mannitol, lactose, raffinose, or trehalose in deionized water). Subsequently, a high-performing Mini Spray Dryer (Dorsa-tech, Iran) was utilized to co-spray dry the mixture. An initial temperature of  $(135 \pm 2)^\circ\text{C}$  was selected after the impact of varying the temperature within the range of  $100^\circ\text{C}$  to  $140^\circ\text{C}$  was studied relying on prior studies.<sup>37-40</sup> The ventilation rate was 800 L/h, and the feed pump rate was 10% (2.5 mL/min), with an aspiration ratio of 80%. Eq. 1 determined the spray drying yield (percent):

$$\text{Yield (\%)} = \frac{\text{Collected dry powder}}{\text{Dry mass in feed solution}} \times 100$$

**Eq. 1**

After collecting powders from the receiving chamber, every sample was kept at room temperature in an effectively labeled glass vial with sealed covers within desiccators for further investigations.

### Characterization of CINA nanoparticles

#### Size distribution of NPs

To determine the size and size distribution of the nanosuspension, we employed the dynamic light scattering technique using Zetasizer X from Malvern Instruments, UK. Prior to the measurement, we diluted a portion of the nanosuspension. The measurements were conducted at

**Table 1.** Factors and the response values of the Box-Behnken design.

Run	Factor 1	Factor 2	Factor 3	Response 1	Response 2
	A: CINA (Con.) (mg/ml)	B: Lecithin (mg)	C: Antisolvent: solvent ratios	Size (Z average) (nm)	PDI (%)
1	140	10	20	1252.7	0.701
2	130	15	20	239.5	0.143
3	120	20	20	499.1	0.581
4	130	15	20	268.3	0.157
5	120	15	30	830.7	0.820
6	130	20	30	765.7	0.822
7	120	10	20	680.3	0.670
8	130	10	30	984.7	0.961
9	120	15	10	624.2	0.714
10	130	15	20	246.1	0.169
11	130	15	20	244.7	0.161
12	130	15	20	264.0	0.201
13	140	15	10	1281.8	0.644
14	130	15	20	257.3	0.189
15	130	10	10	908.6	0.753
16	130	15	20	261.7	0.176
17	130	20	10	734.0	0.712
18	130	15	20	272.7	0.171
19	140	20	20	1004.8	0.590
20	140	15	30	1228.6	0.855

**Table 2.** Design of formulation for the spray drying process.

Run	Factor 1	Factor 2	Response 1	Response 2	Recovery
	A: Amount of sugar (mg)	B: Leucine (%)	Yield (%)	FPF <sub>(ED)</sub> (%)	
1	100	0	22.3	20.1	90.2
2	100	10	25.5	58.2	89.1
3	100	0	22.3	22.1	101.3
4	100	5	23.3	29.2	102.4
5	100	0	21.8	22.9	98.0
6	100	0	22.1	22.5	94.3
7	100	12.5	29.1	76.7	97.3
8	137.5	5	24.7	23.6	91.9
9	137.5	10	27.7	47.5	103.2
10	137.5	5	22.3	25.8	89.9
11	137.5	12.5	30.9	59.3	101.3
12	137.5	0	23.4	20.6	92.7
13	137.5	5	22.3	22.8	104.3
14	137.5	12.5	31.4	64.3	102.5
15	175	0	27.8	18.1	89.1
16	175	0	28.4	17.3	99.6
17	175	5	28.9	22.9	105.2
18	175	10	32.5	39.4	96.2
19	175	10	32.2	38.3	85.4
20	175	12.5	35.7	52.1	83.9

25°C with a dispersion angle of 90 degrees, and we took triplicate readings. The outcomes are presented as the average value  $\pm$  standard deviation (SD).

#### Scanning electron microscopy (SEM)

SEM was used to analyze the morphology and estimated size of particles. To conduct the analysis, powders that were approximately 20 nm thick were affixed to carbon adhesive tape and coated with gold using a BAL-Tec sputter coater (Leica Instruments, Germany). The samples were then examined using a Hitachi S-4160 field emission scanning electron microscope, with an acceleration voltage of 20 kV.

#### Fourier transform infrared spectroscopy (FT-IR)

The Equinox 55 FT-IR spectrophotometer (Bruker, USA) was used to acquire the FT-IR spectra of both the raw CINA and the produced nanocomposite powders. The spectral range of 500 to 3500  $\text{cm}^{-1}$  was investigated with a resolution of 2  $\text{cm}^{-1}$ , utilizing the KBr discs approach. This analysis was performed to identify the molecular structures of raw CINA by comparing the resulting spectra to standard spectra in the literature and to find the possible interaction between stabilizer and drug nanocrystals or possible degradation during the spray-drying process.

#### Differential scanning calorimetry (DSC)

A sample of approximately 7-8 mg of coarse CINA and each of the spray-dried microparticles was weighed and

placed into standard aluminum pans. The pans were then covered carefully. Using a Mettler Toledo 823e differential scanning calorimeter, thermograms were recorded at a heating rate of 10°C/min from 20°C to 200°C. Indium granules and aluminum oxide were used as a standard and reference, respectively.

#### Powder X-ray diffraction (XRD)

To assess the crystallinity of powder samples (raw CINA and processed powders), X-ray powder diffraction was employed. A Bruker AXS D8 advanced X-ray diffractometer (Bruker, USA) was applied to make scans at two theta scales with 1.0° steps at 40 kV and 30 mA Cu-K $\alpha$  radiation.

#### In vitro dissolution studies

In vitro dissolution tests on raw CINA, processed optimum formulation, and a physical mixture of CINA and excipients were performed by a DT6 dissolution tester (Erweka, Germany) using united states pharmacopeia (USP) apparatus II (the paddle method). A known amount (2 mg) of each sample was dispersed in 900 mL phosphate buffer (pH 7.35) at zero time. One-milliliter samples were drawn at determined time intervals (0, 10, 20, 30, 45, and 60 minutes) and the same volume of pre-warmed fresh dissolution medium was replaced. All samples were filtered through a 0.45  $\mu\text{m}$  membrane filter and immediately centrifuged at 13000 rpm for 5 min. Then supernatants



(200 µL) were collected and mixed with an equal volume of methanol. Dissolved drug concentration was measured by HPLC analysis.

### Solubility study

The Higuchi technique was applied to estimate the saturation concentration of the raw CINA and spray-dried CINA samples. In summary, an excessive quantity of sample powders was introduced into a 10 mL phosphate buffer with a pH of 7.4 and deionized water separately in a capped vial and stirred at 300 rpm and 25 °C to ensure the solution reached equilibrium. After 48 h, 1 mL samples were collected and centrifuged at 13000 rpm for 10 min. After diluting the supernatants and filtering them employing a 0.23 µm membrane filter, the HPLC technique was utilized to assess their saturation solubility. The average of the three outcomes from the three repetitions of this experiment was demonstrated.

### In vitro deposition study (aerodynamic data analysis)

To determine the characteristics and pulmonary deposition of spray-dried powders, a twin-stage impinger (TSI) was used. An Aerolizer® inhalation tool (Novartis Pharma) was employed to evaluate the aerodynamic properties of hard gelatin capsules (size 3) containing the amount of optimized spray-dried nanosuspension equivalent to 2.5 mg CINA. The inhalation flow rate through the device was set at  $60 \pm 2$  L/min with a flow duration of 5 seconds. In the HPLC analysis section, the mobile phase suggested was used to sequentially load the upper and lower stages of the TSI with 7 and 30 mL, respectively. An electronic digital flow meter (MKS Instruments, USA) was used to measure the flow. The capsule, device, throat, and upper and lower stages of the twin impinger were rinsed using a specified volume of the mobile phase after actuation. The quantity of CINA deposited in each phase was assessed using the HPLC technique indicated above. Each formulation was tested three times. The formulations' fine particle percentage  $FPF_{ED}$  (%) was estimated as a ratio of particles deposited on stage 2 of TSI to emitted dose  $\times 100$ .

### Stability study

The optimum processed nanocomposite was stored in the screw-capped vial at 40°C and 75%RH for 4 months to analyze drug content, aerodynamic data analysis, and the surface morphology of powders by SEM imaging. Determinations of drug content in formulations were performed on both the bulk powder (total drug content) and processed nanocomposite powder on day zero and followed for 4 months.

## Results

### Preparation and optimization of CINA nanoparticles

For each intended run indicated in Table 1, CINA nanoparticles were produced employing the antisolvent precipitation approach in combination with ultrasonication. As a pretreatment step before sonoprecipitation, the

high shear homogenizing is principally essential for disaggregating large particles. Trial and error among PVA, PVP K30, HPMC, Pluronic F-127, Pluronic F-68, SDS, tween 80, and lecithin at a level of 0.1–0.5 %w/v was employed in this study to determine the proper stabilizer. Preliminary results showed that CINA particles precipitated by adding water to the organic solution of the drug containing relatively low concentrations of lecithin had an appropriate size, and the resulting dispersed system was more stable. Design Expert 11.0.3.0 software was utilized to optimize the formulation parameters and the properties of the resultant powders. The resultant nanoparticles have particle sizes ranging from 239.5 to 1281.8 nm and PDI values ranging from 0.143 to 0.961. The following quadratic models were the best-fitted models for the data:

$$\text{Particle size (nm)} = 256.78 + 266.7 A - 102.83 B + 32.63 C - 16.67 AB - 64.925 AC - 11.1 BC + 372.756 A^2 + 229.681 B^2 + 361.781 C^2 \quad \text{Eq. 2}$$

and

$$\text{PDI} = 0.17087 + 0.000625 A - 0.0475 B + 0.0793 C - 0.0055 AB + 0.02625 AC - 0.0245 BC + 0.205 A^2 + 0.259 B^2 + 0.381 C^2 \quad \text{Eq. 3}$$

Where A indicates the organic phase's concentration of CINA, B denotes the organic phase's concentration of lecithin, and C represents the volume ratio of the aqueous phase to the organic phase. The corrected  $R^2$  (0.9989 for size and 0.9965 for PDI) and the expected  $R^2$  (0.9967 for size and 0.9910 for PDI) agreed well. Optimization was performed for minimum particle size (with five degrees of importance) and minimum PDI (given three degrees of importance). Maximum desirability, 0.99, was observed with a formulation of A = 129.60 mg/mL, B = 15.44 mg, and C = 19.04. After the sonoprecipitation process, the fresh CINA optimum nanosuspension was spray-dried immediately, according to the compositions mentioned in Table 2, and the resulting yield values were recorded.

### Design of spray drying process

In the creation of inhalable CINA microparticles, sugar quantity (mg) (A) and leucine ratio (%) (B) were selected as independent variables in the I-optimal design. Meanwhile, yield (%) and  $FPF_{ED}$  (%) were selected as experimental responses. The relationship between the independent variables and the responses was effectively explained by the quadratic model, with significant results and non-significant lack of fit test in each instance. Eqs. 4 and 5 display the response equations, which are explained in terms of coded factors:

$$\text{Yield\%} = 23.7814 + 1.62911 A + 3.83796 B + 0.254719 AB + 0.23823 A^2 + 3.45976 B^2 \quad \text{Eq. 4}$$

and

$$\text{FPF}_{ED} \% = 28.5665 - 4.75124 A + 24.0049 B - 3.46532 AB + 2.53101 A^2 + 13.6262 B^2 \quad \text{Eq. 5}$$

The ANOVA statistical analysis of each response showed that the model's validity and reliability were consistent, with

the “R-squared” value being close to 1 and the “predicted R-squared” value being close to the “adjusted R-squared.” Table 2 shows the responses and recovery (%) for the suggested formulations. It should be noted that while the drug content statistics are not displayed, determining the drug content was necessary to compute the recovery (%) of each formulation.

Eq. 4 indicates that the leucine ratio (B) has the highest impact on the spray drying yield percentage (%). The lowest yield percentage (%) was obtained with 100 mg of sugar without leucine, as represented in Figure 1A. This suggests that the inclusion of mannitol and leucine in the formulation greatly reduced the powder’s cohesive force, thereby preventing it from sticking to the spray dryer’s walls, and resulted in a high output yield.<sup>41</sup> Eq. 5 and Figure 1B reveal that the leucine ratio (B) had a significant effect on  $FPF_{ED}$  (%).

### Characterization

#### Particle size, zeta potential

All preparations’ observed particle size (nm) and PDI values have been determined, and Table 1 illustrates the results. The optimized preparation yielded  $(239.5 \pm 11.61)$  nm and  $(0.143 \pm 0.0165)$ , respectively. These data indicated

high agreement and statistical equality with the model-predicted particle size values = 239.45 nm and PDI = 0.165. Further, the Zeta potential of the optimum preparation was  $-16.3 \pm 1.6$  mV (Figure 2).

#### Scanning electron microscopy (SEM)

SEM was employed to visualize the surface and particle morphologies (Figures 3a and 3b for the optimized formulation’s nanocomposite and raw CINA, respectively). In contrast to the spray-dried particles, which were spherical with an apparent uniform particle size and a typically smooth surface, the raw CINA powder displayed acicular crystals and a broad particle size variability. Spray-drying the nanosuspensions produced agglomerates that were smoother, less uniform, and less cohesive. Figure 3c exhibits CINA nanocomposite after four months of storage in the mentioned stability study conditions.

#### Fourier transform-infrared spectroscopy (FT-IR) analysis

FT-IR was applied to investigate the potential molecular interactions between CINA and excipients, as well as the degradation of the substance during spray drying. The FT-IR spectra of CINA coarse powder and the CINA nanocomposite made by spray-drying of CINA

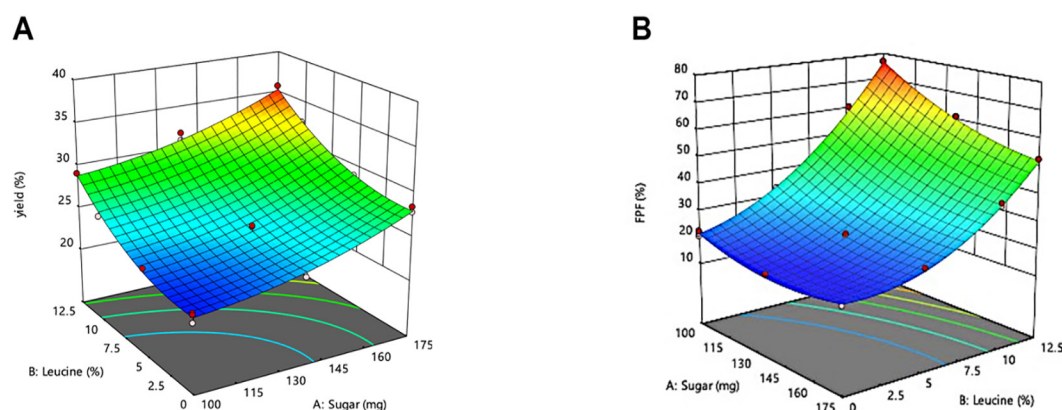


**Figure 1.** The 3D response surface graphs for yield (A) and  $FPF_{ED}$  (%) (B). \*  $FPF_{ED}$ : Fine particle fraction (emitted dose).

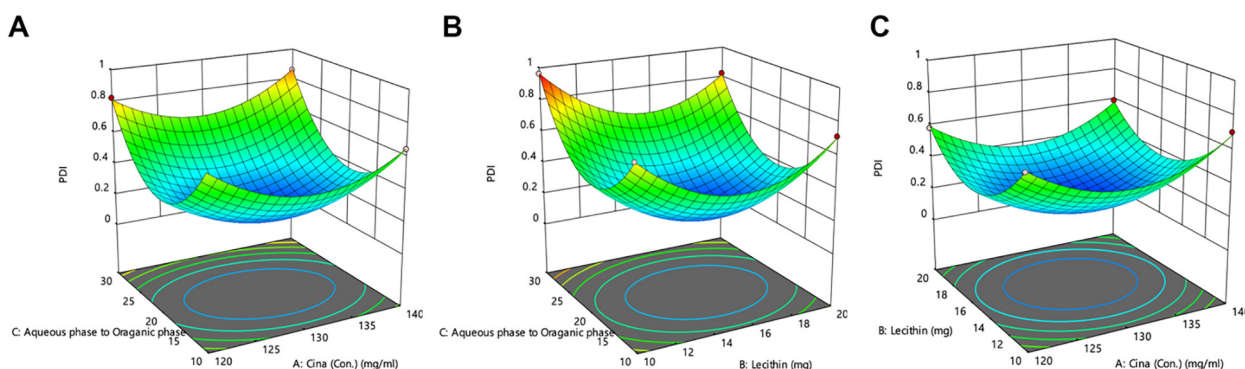


**Figure 2.** The 3D response surface graphs for PDI. (A) The stabilizer (Lecithin) concentration was fixed at 15 mg/ml, (B) The (CINA) concentration was fixed at 130 mg/ml, and (C) The antisolvent/solvent volume ratio was fixed at 20. \*PDI: Polydispersity index.

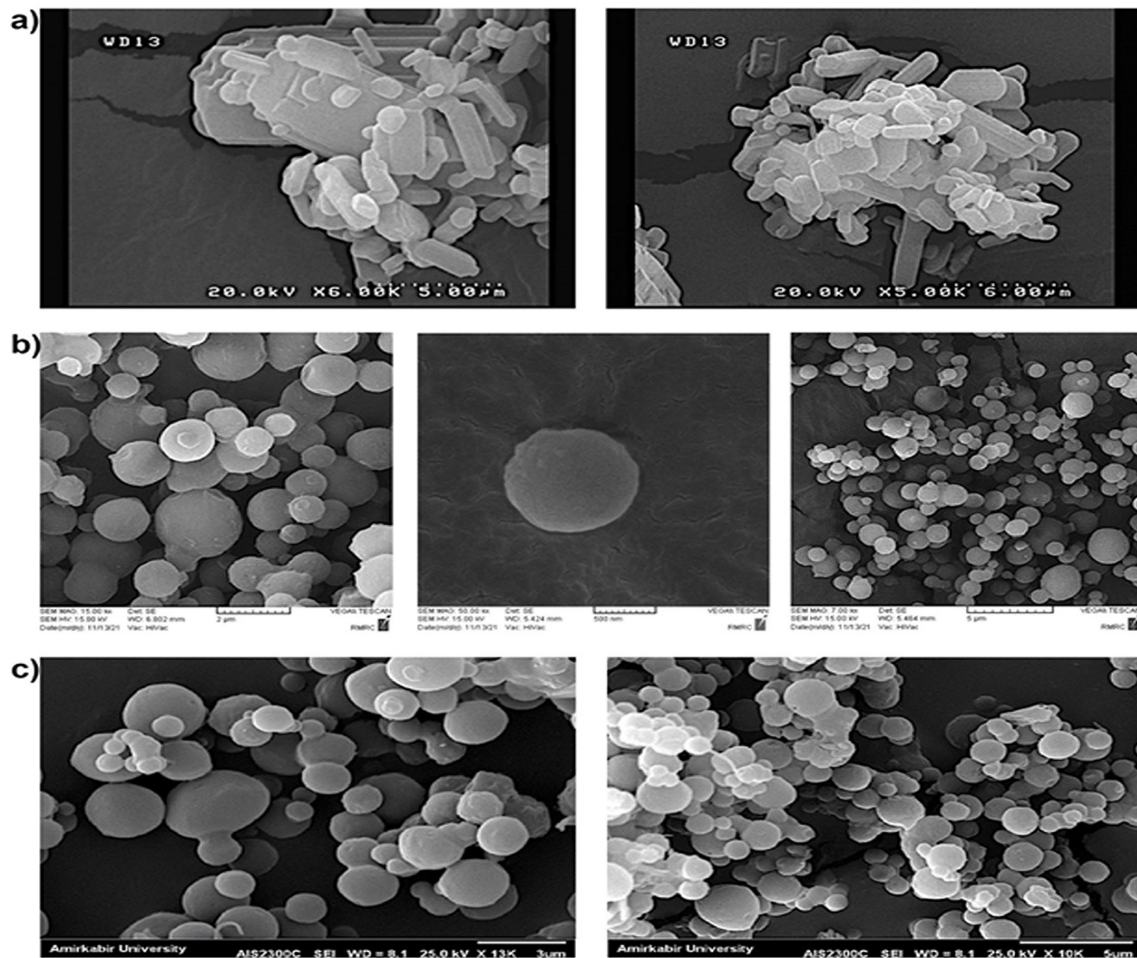


**Figure 3.** SEM micrographs of (a) a raw CINA, (b) CINA nanocomposites prepared under the optimum condition, and (c) CINA nanocomposite after 4 months of storage in the stability mentioned condition.\* SEM: Scanning Electron Microscopy.

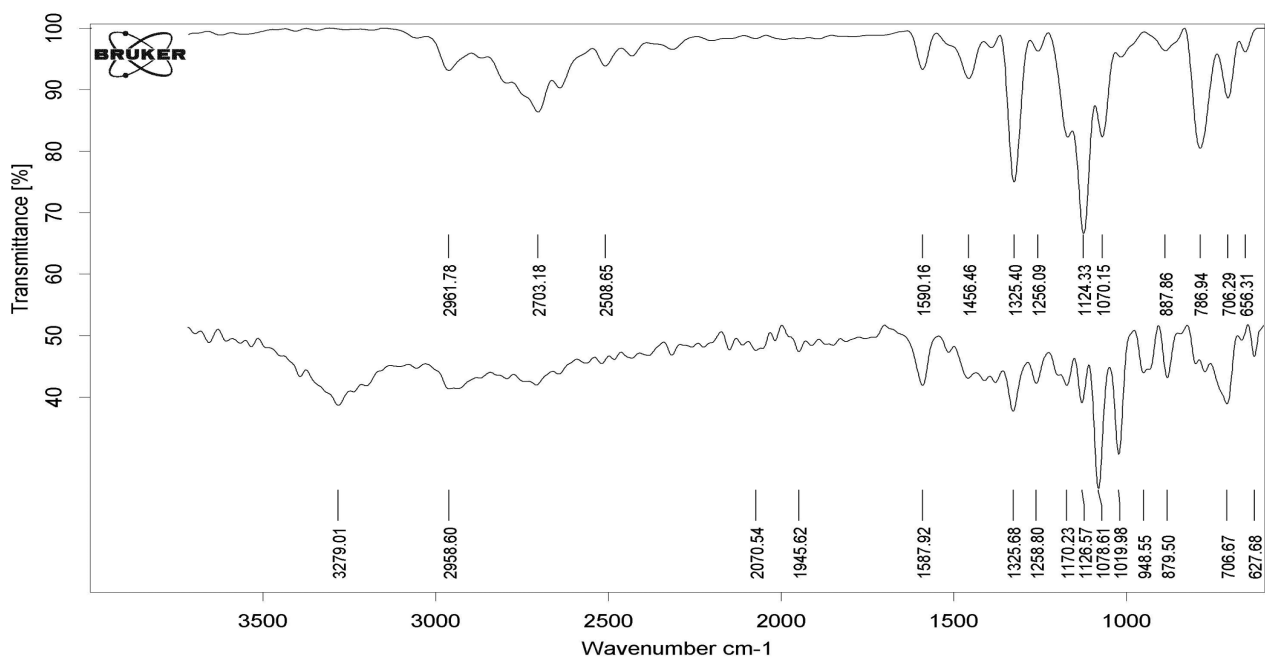


**Figure 4.** Fourier transform-infrared spectra of (a) CINA coarse powder and (b) spray-dried powder of CINA-nanosuspension.

nanosuspension are shown in Figure 4 spectra (a) and (b). The main characteristic peaks of raw CINA were (N–H) stretch  $2961.8\text{ cm}^{-1}$ , aromatic (C–H) stretch  $2797\text{ cm}^{-1}$ , aromatic (C=C) stretch  $1325.4\text{ cm}^{-1}$ , aromatic (C–H) deformation  $788.95\text{ cm}^{-1}$ .

#### Differential scanning calorimetry (DSC)

DSC thermograms could offer important details on the physical condition of nano and microparticles. Figure 5 illustrates how heat flow affects the thermal characteristics

of the coarse CINA and spray-dried powder of CINA nanoparticles. The peak values for processed and coarse CINA were  $162^\circ\text{C}$  and  $182^\circ\text{C}$ , respectively, demonstrating the melting point of CINA. The melting point and enthalpy of the CINA processed powder were lower than those of the coarse CINA, as Figure 5 indicates.

#### X-ray powder diffractometry (XRD)

Powder X-ray diffraction (XRD) was used for evaluating

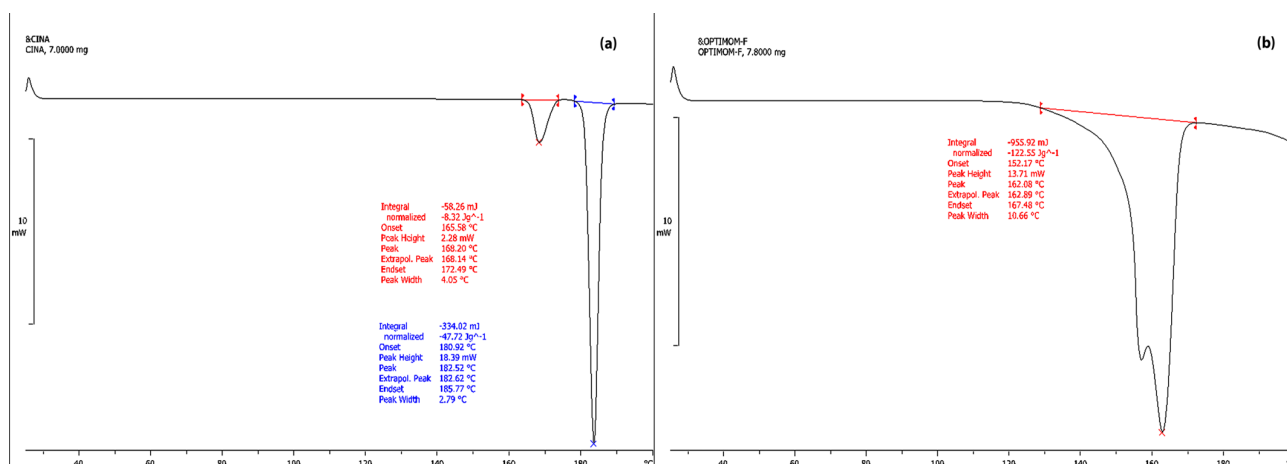


Figure 5. Differential scanning calorimetry thermograms of (a) raw CINA and (b) CINA processed powder.

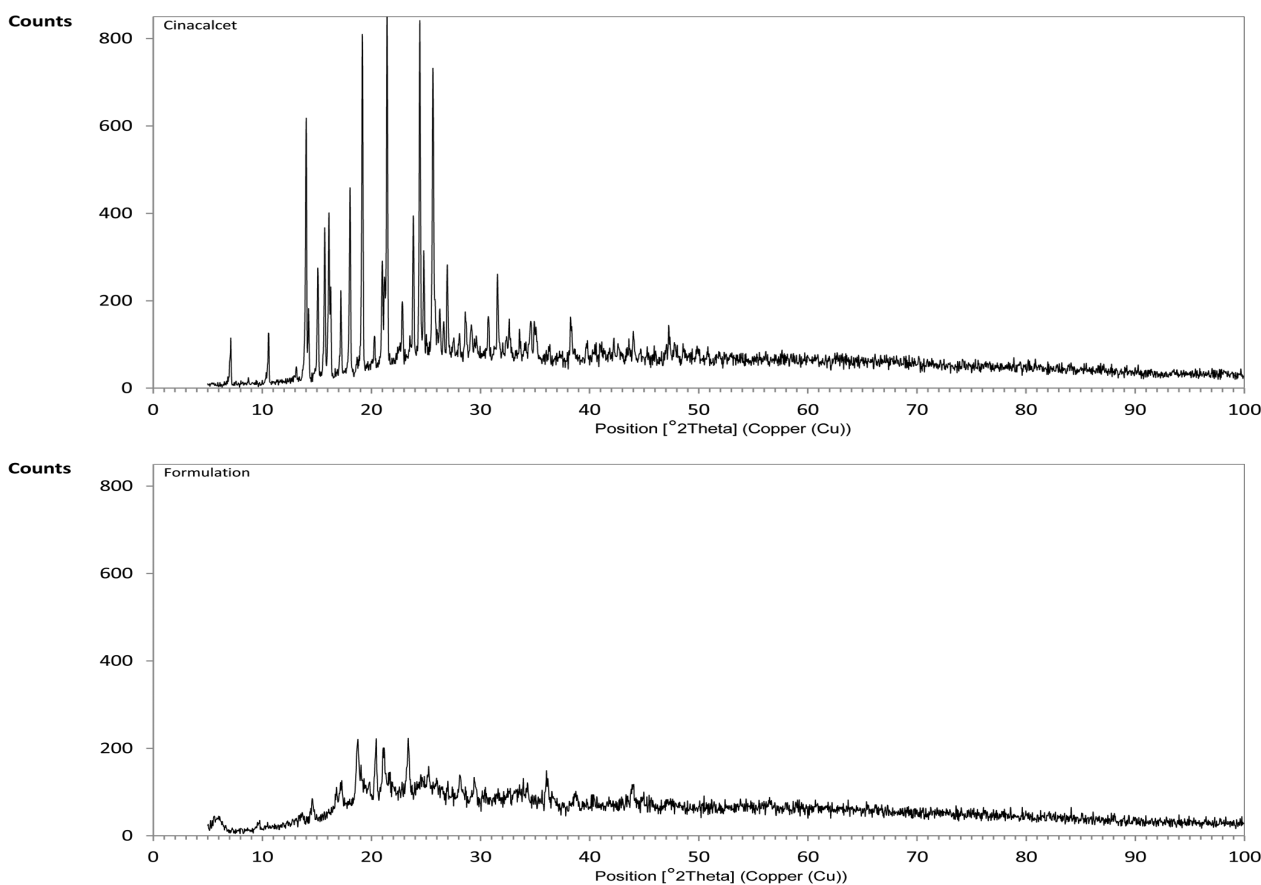


Figure 6. Powder X-ray diffraction patterns of (a) raw CINA and (b) processed CINA.



the crystalline state changes of CINA throughout the processing of the optimized formulation. Measurement samples contained both raw CINA and CINA nanocomposite (Figure 6). The crystalline form of the raw CINA was indicated by its unique peaks, which are depicted in Figure 6 and display the characteristic peaks in  $2\theta$  degrees of  $7^\circ$ ,  $13.1^\circ$ ,  $15.1^\circ$ ,  $16.2^\circ$ ,  $19.1^\circ$ ,  $21^\circ$ ,  $24.4^\circ$ ,  $25.6^\circ$ ,  $30.7^\circ$ ,  $32.6^\circ$ , and  $38.3^\circ$ . Furthermore, the pattern of characteristic peaks of CINA nanocomposite were similar with raw CINA; however lower intensities in diffractogram of CINA nanocomposite are remarkable. This difference could be attributed to a reduction in its crystallinity and a transition towards a partially amorphous state. This phenomenon could potentially be related to either the precipitation or spray drying procedures utilized in its production.

#### Dissolution rate study

Dissolution profiles of pure CINA coarse powder, the physical mixture of formulation components, and the processed nanocomposite are illustrated in Figure 7. Almost 89.95% of the CINA nanocomposite was dissolved in the medium after 45 minutes, as can be exhibited. This was substantially greater ( $p$  value  $< 0.05$ ) than the percentages of raw CINA (14.3%) and the physical combination of CINA and excipients (27.12%). When compared to coarse CINA powder and physical combination, the statistical findings suggested that the drug dissolution from CINA nanocomposite was greater, with a significant difference of  $p < 0.05$  illustrated in all groups.

#### Solubility study

Saturation solubility for each CINA sample was performed over 48 h, and the results of this test are shown in Figure 8.

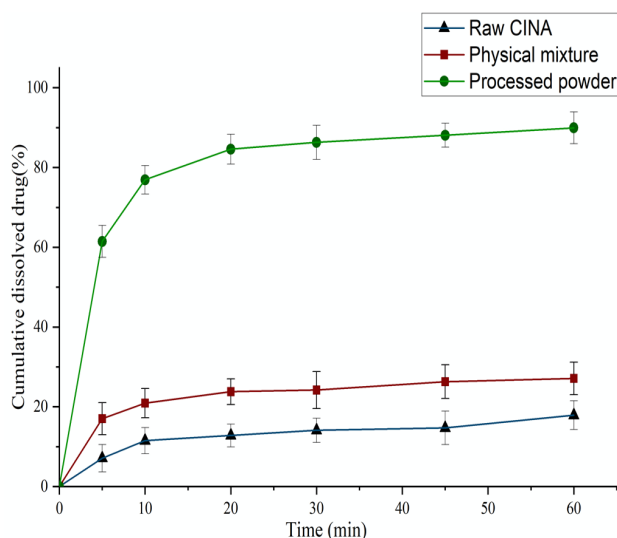


**Figure 7.** The dissolution profiles of raw CINA, physical mixture, and optimum CINA nanocomposite in 900 ml of phosphate buffer (pH=7.4) as dissolution medium, speed rate of 100 rpm and temperature of  $(37 \pm 0.5)^\circ\text{C}$ .

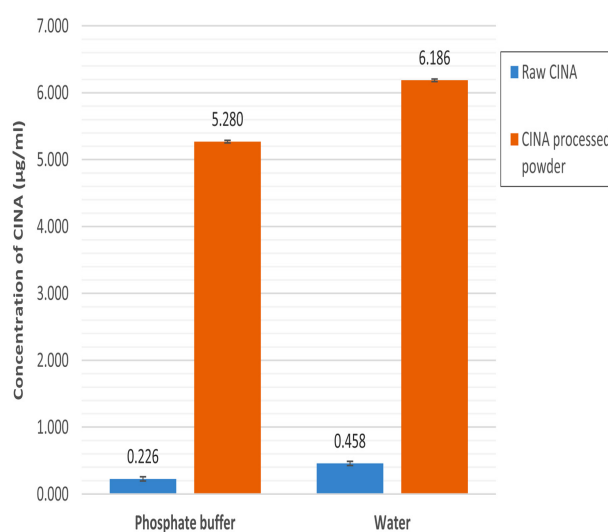
The final solubility of coarse CINA was  $(0.226 \pm 0.015) \mu\text{g/mL}$  in phosphate buffer (pH 7.4) and  $(0.458 \pm 0.031) \mu\text{g/mL}$  in deionized water, whereas that of CINA nanocomposite was  $(5.28 \pm 0.011) \mu\text{g/mL}$  and  $(6.186 \pm 0.02) \mu\text{g/mL}$ , in the mentioned media respectively. That means the saturation solubility of CINA nanocomposites was 23 and 13.5 times more in phosphate buffer and deionized water, respectively.

#### In-vitro aerosol performance (aerodynamic data analysis)

The percentage of fine particles  $\text{FPF}_{\text{ED}} (\%)$  was determined, as well as a quality characteristic determining the aerodynamic performance of a dry powder for inhalation. The synthesized nanoparticle agglomerates possessed  $\text{FPF}_{\text{ED}} (\%)$  values ranging from 17.3 to 76.7% (Table 2). Subsequently, as can be observed in Figures 1A and 1B, the sugar (mannitol) amount (A) of 100 mg and the L-leucine amount (B) of 12.5 mg were found to be the optimum formulation for CINA nanocomposites, which was chosen based on the maximum yield (%) and  $\text{FPF}_{\text{ED}} (\%)$ . The quantities of leucine and mannitol significantly affect the aerodynamic performance of nanoparticle agglomerates. This results in a substantial increase in  $\text{FPF}_{\text{ED}} (\%)$ , from 17.3 % to over 76%. Mannitol's spray-drying capabilities are superior, promoting the creation of spherical particles with a narrow and uniform particle size distribution. Therefore, the beneficial impact of mannitol to drug ratio could be attributed to its ability to create well-defined particles through spray-drying.<sup>42</sup>

#### Stability study

The drug formulation was analyzed for drug content and aerodynamic data analysis after a period of four months. Additionally, SEM analysis was performed to monitor the morphological examination of the surface, as shown in



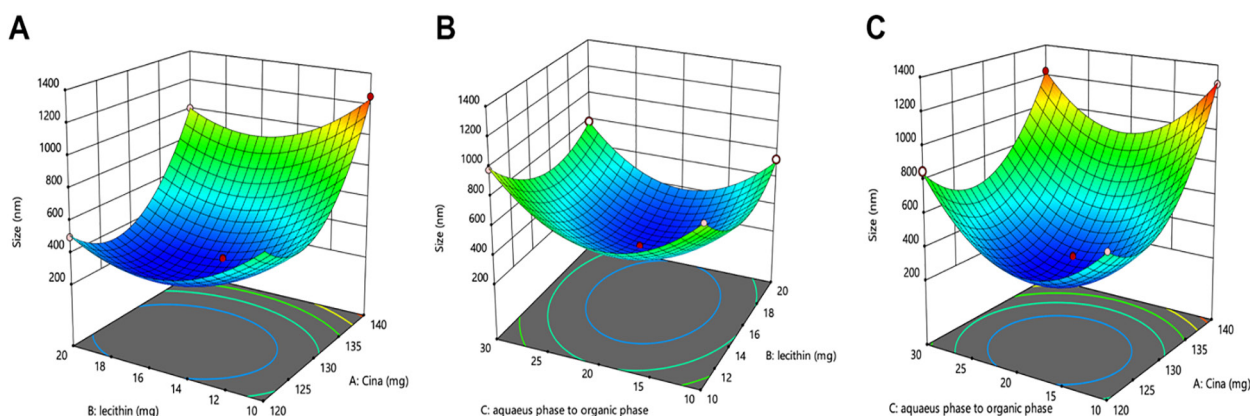
**Figure 8.** The result of saturation solubility of raw CINA and CINA processed powder in two mediums: phosphate buffer (pH=7.4) and deionized water at  $25^\circ\text{C}$ . Each value represents the mean  $\pm$  SD ( $n=3$ ).

Figure 3c. The physicochemical properties of the processed nanocomposite powder remained stable over the four-month period, indicating excellent storage stability of the formulated product.

## Discussion

Precipitation–ultrasonication process was conducted for reduction of drug particle size and to improve sample homogeneity. In this technique, by introducing the drug solution (solvent phase) to an antisolvent phases such as water, which is the most common antisolvent used for hydrophobic drugs like CINA, a high degree of supersaturation occurs, and develops a significant number of nuclei, which lowers the mass of the solute for further development. In this study, ethanol, methanol, DCM, acetone, and DMSO were tested as solvents for the preparations, and DCM was selected due to its high capacity to solubilize CINA (>125 mg/mL). Although ethanol and methanol have the same capacity to solubilize CINA as DCM, formulations based on these two solvents showed aggregations and generated large crystals of CINA. To decrease the free energy of the system consisting of solvent and anti-solvent, suitable stabilizers are utilized in the preparations. Polymers and surfactants are frequently used to prevent medication particles from aggregating through steric, electrostatic, and electrostatic interactions.<sup>24</sup> Due to the decrease in particle size, the particle surface area increases during nanosuspension formation, leading to a boost in the solid-liquid contact area. This rise in the free energy of Gibbs makes the nanosuspensions thermodynamically unstable. This would inevitably result in the aggregation and/or Ostwald's ripening of nanoparticles.<sup>25,43</sup> According to the results, lecithin was selected as the stabilizer because it produced a dispersed system with the appropriate particle size and enhanced stability. Lecithin is commonly applied as a dispersant and surfactant in the complexation process.<sup>44</sup> It is believed that a strong enthalpic interaction (excellent solvation) between the solvent and this stabilizer would have precluded agglomeration by inducing steric repulsion.<sup>24</sup> As a lipid surfactant, lecithin covers the surface

of NCs to produce a steric barrier that keeps NCs and the dispersion medium apart, increasing stability and reducing aggregation. Although a similar result was obtained with SDS, whereas the anionic surfactants may cause irritation or allergic reactions,<sup>45</sup> SDS was excluded from this study. Particle size rose considerably as the concentration of CINA increased, as Figures 9A and 9C indicate. When the drug concentration is increased, more nuclei are generated, and supersaturation develops, initially leading to small particle size. Higher drug concentrations, on the other hand, could result in the creation of greater particles since they accelerate crystal development and encourage coagulation formation of larger particles.<sup>46–48</sup> As illustrated in Figure 9B, the particle size increases by increasing lecithin concentration. In addition, a rising trend in particle size with increasing stabilizer concentration can be noticed in Figure 9A, and it was concluded that, at its optimal concentration, lecithin could effectively encapsulate the surface of the drugs and inhibit particle development through steric stabilization. Excess amounts of surfactant could enwrap the drug particles constantly and cause particle agglomeration due to the bridges formed between particles by Ostwald ripening phenomena.<sup>33,36,49</sup> Furthermore, the volume ratio of the aqueous phase to the organic phase was a significant factor in determining the particulate size of CINA. Therefore, this parameter was evaluated at different antisolvent: solvent ratios (10, 20, 30). The average CINA particle size is affected in two distinct manners by changing the antisolvent: solvent volume ratio, as illustrated in Figures 9B and 9C. Raising the amount of water employed as an antisolvent reduced the solubility of CINA in the mixed solution. It increased supersaturation, which in turn led to a reduction in particle size during recrystallization, all while maintaining a constant concentration of CINA. Among three different antisolvent: solvent ratios tested, preparations of antisolvent: solvent ratio of 20 was more homogenous. On the other hand, a higher antisolvent to the solvent volume would cause particle aggregation due to Ostwald ripening, which is caused by increased CINA nuclei supersaturation.<sup>50,51</sup>



**Figure 9.** The 3D response surface graphs for particle size. (A) The antisolvent: solvent volume ratio was fixed at 20, (B) The (CINA) concentration was set at 130 mg/mL, and (C) The stabilizer (Lecithin) concentration was fixed at 15 mg/mL.

Since nanosuspensions are intrinsically unstable, several drying techniques including spray drying are often used to solidify them to maintain their particle size stability and prevent microbiological growth caused by the aqueous nature of the final medium.<sup>52</sup>

To preserve drugs and enhance their physical stability, excipients like sugars or amino acids may be added as stabilizers. Furthermore, the presence of these sugar molecules in the formulation assists in avoiding particle aggregation during the drying process.<sup>53,54</sup> Less than 3% of the powder was recovered in the CINA nanosuspension scenario due to the majority of the powder sticking to the spray dryer's cyclone. Therefore, the appropriate sugar was chosen by trial and error among four different sugars tested, including lactose, trehalose, raffinose, and mannitol, at different mass ratios. Preliminary results showed that the yield of spray drying of nanosuspensions with trehalose was around 9%, and lactose and raffinose led to a maximum yield of <5% at the highest mass ratio, thus they were excluded from the study.

The reduced yield observed in this study may be attributed to the adherence of the nanoparticle agglomerates to both the drying chamber and cyclone separator. Higher yields were obtained when leucine and mannitol were added to nanosuspension formulations before the spray-drying step. It was discovered that the co-spray drying of leucine with mannitol and trehalose resulted in inadequate discrete particle formation when the leucine content was <5% w/w. As determined in previous studies, a leucine concentration ranging from 5% to 20% w/w was demonstrated to decrease particle aggregation; however, a concentration >20% w/w could enhance surface corrugation.<sup>55</sup> Mannitol has been employed extensively in spray-drying formulations<sup>56</sup> for DPIs and has been demonstrated to have outstanding characteristics since it allows for modifying particle shape and size via process parameter changes.<sup>57</sup> Additionally, mannitol has been applied during the solidification of nanosuspensions due to the formation of a matrix around the microparticle as a water-soluble compound to permit the reformation of the primary nanoparticles when rehydration has occurred.<sup>58,59</sup> It is additionally referred to that some amino acids, such as tri- and L-leucine, improve the aerosol performance of spray-dried DPIs.<sup>60-62</sup> Investigation suggests that co-spraying leucine with API (Active Pharmaceutical Ingredient) enriches leucine on the particle surface and modifies the surface shape of spray-dried particles,<sup>63,64</sup> reducing surface energy and enhancing aerosol performance.<sup>65</sup>

The FT-IR spectra of raw CINA and the CINA nanocomposite exhibited similar peak patterns and frequencies, indicating that the chemical structure of the drug remained unchanged and there was no interaction between the drug and excipients.

To understand the variation of the physicochemical properties of CINA after complexation solid-state characterization of the CINA nanocomposite was investigated. The XRD patterns of the spray-dried

nanocomposite samples as mentioned in results, revealed a diffraction pattern that was comparable to that of CINA, yet with reduced peak intensity, indicating that the processed powder's crystallinity had decreased during the processes.<sup>66</sup> The melting peak in the DSC study shifted towards lower values, which indicates a decrease in CINA crystallinity. This lower melting temperature could be attributed to the existence of some fraction of amorphous state, which may cause a lower melting point.

Combining the data from the DSC and XRD reveals that when preparing nanocrystalline CINA, the crystalline form can alter into a partially amorphous state. The existence of an amorphous fraction in nanocrystals could offer an extra advantage to the drug's dissolving capabilities.<sup>67,68</sup> The results indicated the changes in crystallinity of the drug to a partially amorphous state, which may be possible due to the adhesion of additives, such as surfactants to the surface of nanocrystals<sup>69</sup> or occurred during its production procedures like precipitation and/or spray drying.

Nanoparticles are notable due to their ability to improve the saturation solubility of poorly water-soluble medication. The sonoprecipitation technique, utilized in producing nanocrystals, effectively reduces particle size, resulting in an increased surface area of the solute particles. This, in turn, results in improvements in both solubility and dissolution rate.<sup>70</sup> The results of the experiment revealed that the saturation solubility of the spray-dried nanocomposite of CINA exhibited a quick attainment of maximum solubility, often occurring within the first hour. The insertion of mannitol as a wetting agent and dispersion in the nanocomposite structure leads to a significant improvement in dissolution. This improvement could be attributed to the development of tiny holes in the matrix, which occurs because of the fast dissolution of mannitol. For nanocrystals, the rate of dissolution was significantly increased and plateaued at around 90% in 45 minutes. The greater surface area of the CINA nanocomposite may be primarily responsible for its increased rate of dissolution.<sup>71-73</sup> For nanocrystals, the rate of dissolution was significantly increased and plateaued at around 90% in 45 minutes. The greater surface area of the CINA nanocomposite may be primarily responsible for its increased rate of dissolution.<sup>74,75</sup> Superior dissolution of CINA nanostructures can potentially improve bioavailability and other drug performances.

The NP-agglomerates' spherical form can be detected in the SEM images (Figure 3b). To promote structural cohesiveness, particles with a spherical form and comparatively smooth surfaces might lessen inter-particulate forces such as Van der Waals forces, capillary forces, electrostatic forces, and mechanical interlocking.

The findings demonstrated how leucine altered the characteristics of the resulting spray-dried particles and positively impacted the FPF<sub>ED</sub> (%). Therefore, runs 7 and 14, which had the highest leucine content, possessed the highest FPF<sub>ED</sub> (%), at 76.7% and 64.3%, correspondingly.<sup>76</sup> It has been proven that adding L-leucine to a dry powder

inhaler improves the  $FPF_{ED}$  (%) and aerosolization characteristics by forming an L-leucine shell around the active pharmaceutical ingredient (API) during droplet evaporation, which reduces cohesive forces and improves powder dispersion.<sup>41,77</sup> The FPF revealed that the leucine-to-drug and mannitol-to-drug ratios were the most substantially effective variables. Leucine's beneficial effects may be attributed to its characteristics that improve aerosolization performance and dispersibility. It has also been seen to raise formulations' emissions and fine particle fractions.<sup>78</sup> Leucine significantly and substantially improved the  $FPF_{ED}$  (%) of spray-dried mannitol particles, according to Sou *et al.*<sup>79</sup> More specifically, leucine was discovered to enhance the performance of dry powder inhaler formulations when added to mannitol-based spray dried powder inhalation. This is because leucine forms a coating on the surface of the dry particles, preserving each one as it is collected from the dryer and avoiding any particle adhesion.<sup>58,79</sup> L-leucine has the potential to improve in vitro aerosolization performance and lessen moisture-induced aerosolization deterioration, both of which might contribute to the final product's stability. The quantity of L-leucine causes the main mechanism in the formulation, which relies on the coverage and crystallinity of L-leucine on the surface of particles.<sup>64</sup>

## Conclusion

CINA nanosuspension was successfully prepared using lecithin as the stabilizer, DCM as the solvent, and water as an anti-solvent in a combined methodology of high shear and sonoprecipitation. By conducting an experimental design and optimizing the resultant model, the best formulation was found. When compared to raw CINA, the processed CINA nanocomposites revealed a considerable improvement in solubility and dissolution rate, mainly owing to the reduction in the particle size and transformation to a more amorphous state. Therefore, it appears that selecting the appropriate stabilizers and other excipients, sonoprecipitation and subsequent spray-drying can be applied as a simple and useful approach to produce nanocomposites of CINA. These procedures can be employed on higher scales to produce nanocomposite powders to be utilized in the formulation of oral solid dosage forms or preparations for inhalation. Due to their superior dissolving profile and increased ability to be aerosolized, the NP-agglomerates can be orally administered to the lungs. The primary objective of this study was to deliver drugs to the lungs via NP-agglomerates, and the aerodynamic characteristics suggested that the optimized formula was an effective option for pulmonary administration. Further in vivo pharmacokinetic research is required to determine whether the produced aerosolized CINA nanoparticles are superior to the existing oral CINA drug.

## Author Contributions

Katayoon Mireskandari: Conceptualization, Investigation, Writing - Original Draft, Methodology. Mostafa

Rostamnezhad: Writing - Review & Editing. Majid Darabi: Methodology, Writing - Review & Editing. Mohammadreza Rouini: Conceptualization, Investigation, Supervision, Writing - Review & Editing. Alireza Vatanara: Conceptualization, Investigation, Methodology, Supervision, Writing - Review & Editing.

## Conflict of Interest

The authors report no conflicts of interest.

## References

1. Hickey AJ. Back to the future: inhaled drug products. *J Pharm Sci.* 2013;102(4):1165-72. doi:10.1002/jps.23465
2. Pilcer G, Amighi K. Formulation strategy and use of excipients in pulmonary drug delivery. *Int J Pharm.* 2010;392(1-2):1-19. doi:10.1016/j.ijpharm.2010.03.017
3. Safdar A, Ali Darbandi M. Propranolol micro particle production by spray drying technique and evaluation of the in vitro and in vivo lung deposition. *Interv Cardiol J.* 2016;2(2):14. doi:10.21767/2471-8157.100023
4. Price R, Young PM, Edge S, Staniforth JN. The influence of relative humidity on particulate interactions in carrier-based dry powder inhaler formulations. *Int J Pharm.* 2002;246(1-2):47-59. doi:10.1016/s0378-5173(02)00359-9
5. Salam SN, Khwaja A, Wilkie ME. Pharmacological Management of Secondary hyperparathyroidism in patients with chronic kidney disease. *Drugs.* 2016;76(8):841-52. doi:10.1007/s40265-016-0575-2
6. Nakashima D, Takama H, Ogasawara Y, Kawakami T, Nishitoba T, Hoshi S, et al. Effect of cinacalcet hydrochloride, a new calcimimetic agent, on the pharmacokinetics of dextromethorphan: in vitro and clinical studies. *J Clin Pharmacol.* 2007;47(10):1311-9. doi:10.1177/0091270007304103
7. Komaba H, Nakanishi S, Fujimori A, Tanaka M, Shin J, Shibuya K, et al. Cinacalcet effectively reduces parathyroid hormone secretion and gland volume regardless of pretreatment gland size in patients with secondary hyperparathyroidism. *Clin J Am Soc Nephrol.* 2010;5(12):2305-14. doi:10.2215/CJN.02110310
8. Tominaga Y, Kakuta T, Yasunaga C, Nakamura M, Kadokura Y, Tahara H. Evaluation of parathyroidectomy for secondary and tertiary hyperparathyroidism by the parathyroid surgeons' society of Japan. *Ther Apher Dial.* 2016;20(1):6-11. doi:10.1111/1744-9987.12352
9. Block GA, Martin KJ, de Francisco ALM, Turner SA, Avram MM, Suranyi MG, et al. Cinacalcet for secondary hyperparathyroidism in patients receiving hemodialysis. *N Engl J Med.* 2004;350(15):1516-25. doi:10.1056/NEJMoa031633
10. Gincherman Y, Moloney K, McKee C, Coyne DW. Assessment of adherence to cinacalcet by



- prescription refill rates in hemodialysis patients. *Hemodial Int.* 2010;14(1):68-72. doi:10.1111/j.1542-4758.2009.00397.x
11. Kawata T, Tokunaga S, Murai M, Masuda N, Haruyama W, Shoukei Y, et al. A novel calcimimetic agent, evocalcet (MT-4580/KHK7580), suppresses the parathyroid cell function with little effect on the gastrointestinal tract or CYP isozymes in vivo and in vitro. *PLoS One.* 2018;13(4):e0195316. doi:10.1371/journal.pone.0195316
  12. Padhi D, Harris R. Clinical pharmacokinetic and pharmacodynamic profile of cinacalcet hydrochloride. *Clin Pharmacokinet.* 2009;48(5):303-11. doi:10.2165/00003088-200948050-00002
  13. Cao M, Xue X, Pei X, Qian Y, Liu L, Ren L, et al. Formulation optimization and pharmacokinetics evaluation of oral self-micro emulsifying drug delivery system for poorly water-soluble drug cinacalcet and no food effect. *Drug Dev Ind Pharm.* 2018;44(6):969-81. doi:10.1080/03639045.2018.1425428
  14. Panigrahi KC, Patra CN, Rao MEB. Quality by Design Enabled Development of oral self-nanoemulsifying drug delivery system of a novel calcimimetic cinacalcet hcl using a porous carrier: in vitro and in vivo characterization. *AAPS PharmSciTech.* 2019;20(5):216. doi:10.1208/s12249-019-1411-2
  15. Xu X, Chen G, Li Y, Wang J, Yin J, Ren L. Enhanced dissolution and oral bioavailability of cinacalcet hydrochloride nanocrystals with no food effect. *Nanotechnology.* 2019;30(5):055102. doi:10.1088/1361-6528/aaef46
  16. Routray SB, Patra CN, Raju R, Panigrahi KC, Jena GK. Lyophilized SLN of Cinacalcet HCl: BBD enabled optimization, characterization and pharmacokinetic study. *Drug Dev Ind Pharm.* 2020;46(7):1080-91. doi:10.1080/03639045.2020.1775632
  17. Wang J, Chen GG, Ren LL. Cinacalcet hydrochloride-nanoemulsion: preparation, characterization, enhanced bioavailability and pharmacodynamics. *Eur Rev Med Pharmacol Sci.* 2022;26(8):3010-24. doi:10.26355/eurrev\_202204\_28632
  18. Noyes AA, Whitney WR. The rate of solution of solid substances in their own solutions. *J Am Chem Soc.* 1897;19(12):930-4. doi:10.1021/ja02086a003
  19. Kanikkannan N. Technologies to improve the solubility, dissolution and bioavailability of poorly soluble drugs. *J Anal Pharm Res.* 2018;7(1):00198. doi:10.15406/japlr.2018.07.00198
  20. Singh SK, Srinivasan KK, Gowthamarajan K, Singare DS, Prakash D, Gaikwad NB. Investigation of preparation parameters of nanosuspension by top-down media milling to improve the dissolution of poorly water-soluble glyburide. *Eur J Pharm Biopharm.* 2011;78(3):441-6. doi:10.1016/j.ejpb.2011.03.014
  21. Wang Y, Zheng Y, Zhang L, Wang Q, Zhang D. Stability of nanosuspensions in drug delivery. *J Control Release.* 2013;172(3):1126-41. doi:10.1016/j.jconrel.2013.08.006
  22. Bhakay A, Azad M, Bilgili E, Dave R. Redispersible fast dissolving nanocomposite microparticles of poorly water-soluble drugs. *Int J Pharm.* 2014;461(1-2):367-79. doi:10.1016/j.ijpharm.2013.11.059
  23. Deng Z, Xu S, Li S. Understanding a relaxation behavior in a nanoparticle suspension for drug delivery applications. *Int J Pharm.* 2008;351(1-2):236-43. doi:10.1016/j.ijpharm.2007.10.001
  24. Wu L, Zhang J, Watanabe W. Physical and chemical stability of drug nanoparticles. *Adv Drug Deliv Rev.* 2011;63(6):456-69. doi:10.1016/j.addr.2011.02.001
  25. Van Eerdenbrugh B, Van den Mooter G, Augustijns P. Top-down production of drug nanocrystals: nanosuspension stabilization, miniaturization and transformation into solid products. *Int J Pharm.* 2008;364(1):64-75. doi:10.1016/j.ijpharm.2008.07.023
  26. Patravale VB, Date AA, Kulkarni RM. Nanosuspensions: a promising drug delivery strategy. *J Pharm Pharmacol.* 2004;56(7):827-40. doi:10.1211/0022357023691
  27. Chaubal MV, Popescu C. Conversion of nanosuspensions into dry powders by spray drying: a case study. *Pharm Res.* 2008;25(10):2302-8. doi:10.1007/s11095-008-9625-0
  28. Abdelwahed W, Degobert G, Stainmesse S, Fessi H. Freeze-drying of nanoparticles: formulation, process and storage considerations. *Adv Drug Deliv Rev.* 2006;58(15):1688-713. doi:10.1016/j.addr.2006.09.017
  29. Stepankova V, Bidmanova S, Koudelakova T, Prokop Z, Chaloupkova R, Damborsky J. Strategies for stabilization of enzymes in organic solvents. *ACS Catal.* 2013;3(12):2823-36. doi:10.1021/cs400684x
  30. Sun W, Ni R, Zhang X, Li LC, Mao S. Spray drying of a poorly water-soluble drug nanosuspension for tablet preparation: formulation and process optimization with bioavailability evaluation. *Drug Dev Ind Pharm.* 2015;41(6):927-33. doi:10.3109/03639045.2014.914528
  31. Mansour HM, Rhee YS, Wu X. Nanomedicine in pulmonary delivery. *Int J Nanomedicine.* 2009;4:299-319. doi:10.2147/ijn.s4937
  32. Xi J, Longest PW. Effects of oral airway geometry characteristics on the diffusional deposition of inhaled nanoparticles. *J Biomech Eng.* 2008;130(1):011008. doi:10.1115/1.2838039
  33. Kesisoglou F, Panmai S, Wu Y. Nanosizing--oral formulation development and biopharmaceutical evaluation. *Adv Drug Deliv Rev.* 2007;59(7):631-44. doi:10.1016/j.addr.2007.05.003
  34. Hu J, Ng WK, Dong Y, Shen S, Tan RBH. Continuous and scalable process for water-redispersible nano formulation of poorly aqueous soluble APIs by antisolvent precipitation and spray-drying. *Int J Pharm.* 2011;404(1-2):198-204. doi:10.1016/j.ijpharm.2010.10.055
  35. Jeong YI, Shim YH, Kim C, Lim GT, Choi KC, Yoon

- C. Effect of cryoprotectants on the reconstitution of surfactant-free nanoparticles of poly (DL-lactide-co-glycolide). *J Microencapsul.* 2005;22(6):593-601. doi:10.1080/02652040500162659
36. Liu D, Xu H, Tian B, Yuan K, Pan H, Ma S, et al. Fabrication of carvedilol nanosuspensions through the anti-solvent precipitation-ultrasonication method for the improvement of dissolution rate and oral bioavailability. *AAPS PharmSciTech.* 2012;13(1):295-304. doi:10.1208/s12249-011-9750-7
  37. Seville PC, Li HY, Learoyd TP. Spray-dried powders for pulmonary drug delivery. *Crit Rev Ther Drug Carrier Syst.* 2007;24(4):307-60. doi:10.1615/critrevtherdrugcarriersyst.v24.i4.10
  38. Littringer EM, Mescher A, Eckhard S, Schröttner H, Langes C, Fries M, et al. Spray Drying of Mannitol as a Drug Carrier—The Impact of Process Parameters on Product Properties. *Drying Technol.* 2012;30(1):114-24. doi:10.1080/07373937.2011.620726
  39. Kumar S, Jog R, Shen J, Zolnik B, Sadrieh N, Burgess DJ. Formulation and performance of danazol nanocrystalline suspensions and spray dried powders. *Pharm Res.* 2015;32(5):1694-703. doi:10.1007/s11095-014-1567-0
  40. Pilcer G, Vanderbist F, Amighi K. Preparation and characterization of spray-dried tobramycin powders containing nanoparticles for pulmonary delivery. *Int J Pharm.* 2009;365(1-2):162-9. doi:10.1016/j.ijpharm.2008.08.014
  41. Rattanupatam T, Srichana T. Budesonide dry powder for inhalation: effects of leucine and mannitol on the efficiency of delivery. *Drug Deliv.* 2014;21(6):397-405. doi:10.3109/10717544.2013.868555
  42. Li X, Vogt FG, Hayes D Jr, Mansour HM. Design, characterization, and aerosol dispersion performance modeling of advanced co-spray dried antibiotics with mannitol as respirable microparticles/nanoparticles for targeted pulmonary delivery as dry powder inhalers. *J Pharm Sci.* 2014;103(9):2937-49. doi:10.1002/jps.23955
  43. Jacob S, Nair AB, Shah J. Emerging role of nanosuspensions in drug delivery systems. *Biomater Res.* 2020;24:3. doi:10.1186/s40824-020-0184-8
  44. Salazar J, Ghanem A, Müller RH, Möschwitzer JP. Nanocrystals: comparison of the size reduction effectiveness of a novel combinative method with conventional top-down approaches. *Eur J Pharm Biopharm.* 2012;81(1):82-90. doi:10.1016/j.ejpb.2011.12.015
  45. Liversidge GG, Cundy KC. Particle size reduction for improvement of oral bioavailability of hydrophobic drugs: I. Absolute oral bioavailability of nanocrystalline danazol in beagle dogs. *Int J Pharm.* 1995;125(1):91-7. doi:10.1016/0378-5173(95)00122-Y
  46. Xia D, Quan P, Piao H, Piao H, Sun S, Yin Y, et al. Preparation of stable nitrendipine nanosuspensions using the precipitation-ultrasonication method for enhancement of dissolution and oral bioavailability. *Eur J Pharm Sci.* 2010;40(4):325-34. doi:10.1016/j.ejps.2010.04.006
  47. Kakran M, Sahoo NG, Li L, Judeh Z, Wang Y, Chong K, et al. Fabrication of drug nanoparticles by evaporative precipitation of nanosuspension. *Int J Pharm.* 2010;383(1-2):285-92. doi:10.1016/j.ijpharm.2009.09.030
  48. Zhang HX, Wang JX, Zhang ZB, Le Y, Shen ZG, Chen JF. Micronization of atorvastatin calcium by antisolvent precipitation process. *Int J Pharm.* 2009;374(1-2):106-13. doi:10.1016/j.ijpharm.2009.02.015
  49. Chen JF, Zhou MY, Shao L, Wang YY, Yun J, Chew NYK, et al. Feasibility of preparing nanodrugs by high-gravity reactive precipitation. *Int J Pharm.* 2004;269(1):267-74. doi:10.1016/j.ijpharm.2003.09.044
  50. Lee AY, Lee IS, Dette SS, Boerner J, Myerson AS. Crystallization on confined engineered surfaces: a method to control crystal size and generate different polymorphs. *J Am Chem Soc.* 2005;127(43):14982-3. doi:10.1021/ja055416x
  51. Zu Y, Li N, Zhao X, Li Y, Ge Y, Wang W, et al. In vitro dissolution enhancement of micronized l-nimodipine by antisolvent re-crystallization from its crystal form H. *Int J Pharm.* 2014;464(1-2):1-9. doi:10.1016/j.ijpharm.2014.01.020
  52. Kobierski S, Ofori-Kwakye K, Müller RH, Keck CM. Resveratrol nanosuspensions: interaction of preservatives with nanocrystal production. *Pharmazie.* 2011;66(12):942-7. doi:10.1691/ph.2011.1038
  53. Kumar S, Gokhale R, Burgess DJ. Sugars as bulking agents to prevent nano-crystal aggregation during spray or freeze-drying. *Int J Pharm.* 2014;471(1-2):303-11. doi:10.1016/j.ijpharm.2014.05.060
  54. Layre AM, Couvreur P, Richard J, Requier D, Eddine Ghermani N, Gref R. Freeze-drying of composite core-shell nanoparticles. *Drug Dev Ind Pharm.* 2006;32(7):839-46. doi:10.1080/03639040600685134
  55. Sou T, Kaminskas LM, Nguyen TH, Carlberg R, McIntosh MP, Morton DAV. The effect of amino acid excipients on morphology and solid-state properties of multi-component spray-dried formulations for pulmonary delivery of biomacromolecules. *Eur J Pharm Biopharm.* 2013;83(2):234-43. doi:10.1016/j.ejpb.2012.10.015
  56. Rahimpour Y, Kouhsoltani M, Hamishehkar H. Alternative carriers in dry powder inhaler formulations. *Drug Discov Today.* 2014;19(5):618-26. doi:10.1016/j.drudis.2013.11.013
  57. Maas SG, Schaldach G, Littringer EM, Mescher A, Griesser UJ, Braun DE, et al. The impact of spray drying outlet temperature on the particle morphology of mannitol. *Powder Technol.* 2011;213(1):27-35. doi:10.1016/j.powtec.2011.06.024
  58. Malamatar M, Somavarapu S, Bloxham M, Buckton G. Nanoparticle agglomerates of indomethacin: The role of poloxamers and matrix former on

- their dissolution and aerosolization efficiency. *Int J Pharm.* 2015;495(1):516-26. doi:10.1016/j.ijpharm.2015.09.013
59. Yamasaki K, Kwok PCL, Fukushima K, Prud'homme RK, Chan HK. Enhanced dissolution of inhalable cyclosporine nano-matrix particles with mannitol as matrix former. *Int J Pharm.* 2011;420(1):34-42. doi:10.1016/j.ijpharm.2011.08.010
  60. Arora S, Haghi M, Young PM, Kappl M, Traini D, Jain S. Highly respirable dry powder inhalable formulation of voriconazole with enhanced pulmonary bioavailability. *Expert Opin Drug Deliv.* 2016;13(2):183-93. doi:10.1517/17425247.2016.1114603
  61. Chow AHL, Tong HHY, Chattopadhyay P, Shekunov BY. Particle engineering for pulmonary drug delivery. *Pharm Res.* 2007;24(3):411-37. doi:10.1007/s11095-006-9174-3
  62. Lechuga-Ballesteros D, Charan C, Stults CLM, Stevenson CL, Miller DP, Vehring R, et al. Trileucine improves aerosol performance and stability of spray-dried powders for inhalation. *J Pharm Sci.* 2008;97(1):287-302. doi:10.1002/jps.21078
  63. Boraey MA, Hoe S, Sharif H, Miller DP, Lechuga-Ballesteros D, Vehring R. Improvement of the dispersibility of spray-dried budesonide powders using leucine in an ethanol-water cosolvent system. *Powder Technol.* 2013;236:171-8. doi:10.1016/j.powtec.2012.02.047
  64. Li L, Sun S, Parumasivam T, Denman JA, Gengenbach T, Tang P, et al. L-Leucine as an excipient against moisture on in vitro aerosolization performances of highly hygroscopic spray-dried powders. *Eur J Pharm Biopharm.* 2016;102:132-41. doi:10.1016/j.ejpb.2016.02.010
  65. Chaudhary KR, Singh K, Singh C. Recent updates in inhalable drug delivery system against various pulmonary diseases: challenges and future perspectives. *Curr Drug Deliv.* 2023. doi:10.2174/0115672018265571231011093546
  66. Kumar BS, Saraswathi R, Kumar KV, Jha SK, Venkates DP, Dhanaraj SA. Development and characterization of lecithin stabilized glibenclamide nanocrystals for enhanced solubility and drug delivery. *Drug Deliv.* 2014;21(3):173-84. doi:10.3109/10717544.2013.840690
  67. Morakul B, Suksiriworapong J, Chomnawang MT, Langguth P, Junyaprasert VB. Dissolution enhancement and in vitro performance of clarithromycin nanocrystals produced by precipitation-lyophilization-homogenization method. *Eur J Pharm Biopharm.* 2014;88(3):886-96. doi:10.1016/j.ejpb.2014.08.013
  68. Keck CM, Müller RH. Drug nanocrystals of poorly soluble drugs produced by high pressure homogenisation. *Eur J Pharm Biopharm.* 2006;62(1):3-16. doi:10.1016/j.ejpb.2005.05.009
  69. Hecq J, Deleers M, Fanara D, Vranckx H, Amighi K. Preparation and characterization of nanocrystals for solubility and dissolution rate enhancement of nifedipine. *Int J Pharm.* 2005;299(1-2):167-77. doi:10.1016/j.ijpharm.2005.05.014
  70. Sun J, Wang F, Sui Y, She Z, Zhai W, Wang C, et al. Effect of particle size on solubility, dissolution rate, and oral bioavailability: evaluation using coenzyme Q10 as naked nanocrystals. *Int J Nanomedicine.* 2012;7:5733-44. doi:10.2147/IJN.S34365
  71. Azad M, Arteaga C, Abdelmalek B, Davé R, Bilgili E. Spray drying of drug-swellable dispersant suspensions for preparation of fast-dissolving, high drug-loaded, surfactant-free nanocomposites. *Drug Dev Ind Pharm.* 2015;41(10):1617-31. doi:10.3109/03639045.2014.976574
  72. Davis M, Walker G. Recent strategies in spray drying for the enhanced bioavailability of poorly water-soluble drugs. *J Control Release.* 2018;269:110-27. doi:10.1016/j.jconrel.2017.11.005
  73. Duret C, Wauthoz N, Sebti T, Vanderbist F, Amighi K. New inhalation-optimized itraconazole nanoparticle-based dry powders for the treatment of invasive pulmonary aspergillosis. *Int J Nanomedicine.* 2012;7:5475-89. doi:10.2147/IJN.S34091
  74. Kocbek P, Baumgartner S, Kristl J. Preparation and evaluation of nanosuspensions for enhancing the dissolution of poorly soluble drugs. *Int J Pharm.* 2006;312(1-2):179-86. doi:10.1016/j.ijpharm.2006.01.008
  75. Dong Y, Ng WK, Hu J, Shen S, Tan RBH. A continuous and highly effective static mixing process for antisolvent precipitation of nanoparticles of poorly water-soluble drugs. *Int J Pharm.* 2010;386(1-2):256-61. doi:10.1016/j.ijpharm.2009.11.007
  76. Hickey AJ, Mansour HM, Telko MJ, Xu Z, Smyth HDC, Mulder T, et al. Physical characterization of component particles included in dry powder inhalers. I. Strategy review and static characteristics. *J Pharm Sci.* 2007;96(5):1282-301. doi:10.1002/jps.20916
  77. Molina C, Kaialy W, Nokhodchi A. The crucial role of leucine concentration on spray dried mannitol-leucine as a single carrier to enhance the aerosolization performance of Albuterol sulfate. *J Drug Deliv Sci Technol.* 2019;49:97-106. doi:10.1016/j.jddst.2018.11.007
  78. Seville PC, Learoyd TP, Li HY, Williamson IJ, Birchall JC. Amino acid-modified spray-dried powders with enhanced aerosolisation properties for pulmonary drug delivery. *Powder Technol.* 2007;178(1):40-50. doi:10.1016/j.powtec.2007.03.046
  79. Sou T, Orlando L, McIntosh MP, Kaminskas LM, Morton DAV. Investigating the interactions of amino acid components on a mannitol-based spray-dried powder formulation for pulmonary delivery: A design of experiment approach. *Int J Pharm.* 2011;421(2):220-9. doi:10.1016/j.ijpharm.2011.09.018